Acta Crystallographica Section A
Foundations of Crystallography
ISSN 0108-7673

Received 2 August 2005
Accepted 2 November 2005

X-ray diffraction by a crystal in a permanent external electric field: electric-field-induced structural response in α-$GaPO_4$

Semen Gorfman,[a,b] Vladimir Tsirelson,[b,a] Andreas Pucher,[a] Wolfgang Morgenroth[c] and Ullrich Pietsch[a]*

[a]Institute of Physics, University of Potsdam, Germany, [b]Quantum Chemistry Department, Mendeleev University of Chemical Technology, Moscow, Russia, and [c]HASYLAB at DESY, Hamburg, Germany. Correspondence e-mail: upietsch@gadir.physik.uni-potsdam.de

For the first time, site-selective distortion has been investigated for two different structural units in the ternary compound α-$GaPO_4$ under the influence of a permanent external electric field. Based on 54 measured reflection intensities, the electric-field-induced distortion of PO_4 and GaO_4 tetrahedra in α-$GaPO_4$ crystals is evaluated using a model of pseudoatomic displacements introduced recently [Gorfman, Tsirelson & Pietsch (2005). *Acta Cryst.* A**61**, 387–396]. A stronger variation of the P—O bond lengths in the PO_4 tetrahedron was found compared to the bonds in the GaO_4 tetrahedron. The different distortions of the tetrahedra owing to the electric field were analysed in terms of the valence charge density of α-$GaPO_4$ and its topological characteristics. The larger charge of the P pseudoatom compared to the Ga atom was recognized as the main reason for the higher sensitivity of the PO_4 tetrahedron to a permanent external electric field.

1. Introduction

In recent years, X-ray diffraction structural analysis, which allows deriving and analysing electron density and thermal motion in crystals, has been greatly improved (Tsirelson & Ozerov, 1996). This progress can be characterized by three major steps: (i) the improvement in accuracy of measured X-ray diffraction intensities collected at synchrotron-radiation sources; (ii) the development of models for reconstructing the quasistatic electron density based on the multipole model (Coppens, 1997); and (iii) the quantum-mechanical analysis of bonding based on the theory of atoms in molecules (Bader, 1990). After these achievements, the study of the structural response of electron and nuclear systems of a crystal to any distortion of the equilibrium becomes very attractive. In addition to the temperature and other nearly isotropic external perturbations, like hydrostatic pressure, the study of structural distortions in crystals under an external electric field (*E*-field) is most interesting. The experimental methods applied for this purpose are described by Aslanov *et al.* (1989), Graafsma *et al.* (1992, 1998), Stahn *et al.* (1998, 2001), Davaasambuu *et al.* (2003) and Guillot *et al.* (2004).

Gorfman *et al.* (2005) (hereafter referred to as paper I) and Tsirelson *et al.* (2003) have recently undertaken a theoretical study of a crystal response to an external *E*-field in terms of the quantities derivable from an X-ray diffraction experiment. It has been shown that the variations in X-ray diffraction pattern induced by an external *E*-field are mainly related to the displacements of rigid pseudoatomic fragments from their equilibrium field-free positions. In the present work, we apply the X-ray diffraction technique to the study of *E*-field-induced pseudoatomic displacements in a gallium phosphate crystal, α-$GaPO_4$. This ternary compound is isostructural to α-quartz and shows an alternative arrangement of GaO_4 and PO_4

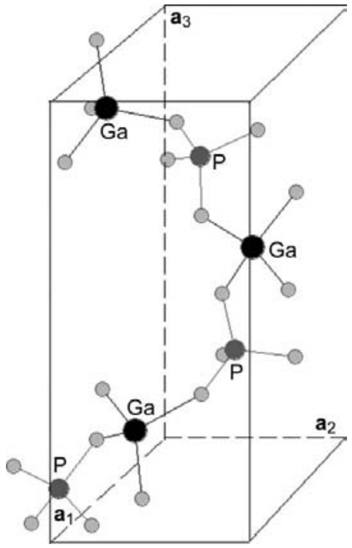

Figure 1
The atomic structure of α-$GaPO_4$.

doi:10.1107/S0108767305036111

tetrahedra along the direction of the hexagonal a_3 axis (Fig. 1). The structural distortions in α-quartz under an external E-field were studied by X-ray diffraction techniques (Davaasambuu, 2003) and by theoretical density functional calculations (Kochin *et al.*, 2004). It was shown that the distortion can be approximately described as rotations of nearly rigid structural tetrahedra against each other. The same conclusion was achieved in a number of high-pressure X-ray diffraction studies of α-quartz (Hazen *et al.*, 1989; Glinnemann *et al.*, 1992). On the other hand, Guillot *et al.* (2004) have shown that accounting for small bond-length variations and intra-tetrahedron angles improves the agreement between simulated and measured X-ray diffraction intensities. Owing to the isomorphic character of the α-GaPO$_4$ and α-SiO$_2$ structures, the response of gallium phosphate as a whole to an external E-field might be comparable to that for α-quartz. At the same time, one may expect that the GaO$_4$ and PO$_4$ tetrahedra will react differently to an external E-field owing to the difference in the P—O and Ga—O bonding. The purpose of the present investigation is to probe the different sensitivities of these structural units to an external electric field and to find an explanation in terms of the different characteristics of the chemical bonds.

The procedure of the measurement of X-ray diffraction intensities in an external E-field is very expensive and time consuming. In order to analyse small variations of the reflected intensity, one has to collect a sufficient count number, n, providing a Poisson error, $\sigma = 1/n^{1/2}$, of order 0.2%. Such good counting statistics cannot be achieved with a laboratory X-ray tube and weak reflections; therefore we have performed the experiment at beamline D3 at the Hamburg Synchrotron Laboratory (HASYLAB). Even at a synchrotron-radiation source, only a few reflections can be collected during a reasonable beamtime (*ca* 1 week), therefore the reflections, measured in the presence of the external E-field, were carefully selected on the basis of the theory described in paper I. There we proposed an analytical expression that can be used to estimate an E-field-induced intensity variation for an arbitrary reflection and to choose those most sensitive to an external E-field. Applying such a strategy for the diffraction experiment, we can reduce the experimental effort to the measurement of those reflections that carry the maximum information about electric-field-induced atomic displacements.

In §2, we describe the X-ray diffraction experiment with a crystal under external electric field. §3 introduces the models for data analysis; here the results obtained in paper I are applied to gallium phosphate. §4 deals with the least-squares methods applied to different models for the measured variations of X-ray diffraction intensities induced by an external E-field. In §5, we consider the physical validity of the pseudoatomic displacements and examine whether the macroscopic dielectric properties can be reproduced on the basis of the pseudoatomic model of the electron density. Finally, we analyse the distortion of both of the tetrahedral units and discuss the obtained results in terms of the respective bond characteristics.

2. Sample preparation and measurement technique

The α-GaPO$_4$ crystals in the right-hand modification (space group $P3_121$) were purchased from the Piezocryst Company (Austria). Plane wafer-shaped crystals with a thickness of 0.3 mm and a typical surface area of 1.0 cm^2 were cut parallel to the Miller planes (110) (X cut) and (100) (Y cut). The wafer faces were polished and thin silver contacts, being transparent to the X-rays, were deposited on both faces thus allowing the application of an external voltage.

The modulation–demodulation X-ray diffraction technique described by Puget & Godefroy (1975), Fujimoto (1982), Stahn *et al.* (2001), van Reeuwijk (2002) and Guillot *et al.* (2004) was used to measure the E-field-induced response of the crystal structure. The room-temperature measurements of X-ray intensities were carried out at the D3 bending magnet beamline at HASYLAB equipped with a Huber four-circle goniometer. After determination of the orientation matrix of the samples, a series of rocking curves was recorded in the ω-scan mode for reflections selected according to the procedure described in paper I. The periodically varying external field was applied along the surface normal to the respective wafer and the intensities were separately recorded into three different detector channels correspondingly for positive, zero and negative voltage. The time of charging/discharging the sample capacity after the switching of the external voltage from one value to another was excluded from the data recording. The duration of the external modulation/demodulation signal was 10 ms, which is long enough to consider the applied voltage as permanent and short enough to avoid the accumulation of screening charges at both sample surfaces and crystal defects. Another purpose of an external E-field modulation is the opportunity of quasisimultaneous measurements of three different rocking curves corresponding to the values of an external E-field (positive, zero, negative). Therefore, the evaluated intensity differences of the measured rocking curves are little affected by instabilities of experimental equipment and beam intensity.

The wavelength of a primary X-ray beam was set by a double-crystal Si (111) monochromator. The ability of a flexible wavelength choice is important in the study of α-GaPO$_4$ since the K-absorption edge of gallium (λ_K = 1.19 Å) is accessible in this case. As shown in paper I, the sensitivity of a reflection with respect to an external E-field can be maximized by tuning a wavelength to a value close to the K-absorption edge. For the data treatment, only rocking curves that were free from multiple scattering (*Umweganregung*) were further considered. The absence of multiple scattering was checked by ω scans at different ψ angles.

In order to distinguish between the $(11\bar{2}0)$ and $(\bar{1}\bar{1}20)$ faces of the sample (for the X-cut case), we measured the piezoelectric shift of an angular peak position, θ, related to the change of crystal lattice parameters (external piezoelectric effect) and, therefore, to the piezoelectric coefficients d_{ijk}:

$$\Delta\theta = -\tan\theta \, d_{ijk} E_i H_j H_k / H^2, \qquad (1)$$

E_i and H_i are, respectively, the components of an external E-field vector and the reciprocal-lattice vector in a Cartesian system associated with the specific crystallographic setting (Nye, 2004). Comparing the signs of the calculated and observed peak shifts, we determined the correct orientation of the polar axes relative to an external E-field. The piezoelectric coefficients in the right-hand modification of α-GaPO$_4$ were taken from Krispel *et al.* (1997).

The rocking curves for each measured reflection were scanned over *ca* 100 points of the ω-circle positions. The scan range was chosen to integrate the intensity with sufficient accuracy and to measure the background level accurately. The observed X-ray diffraction intensities were reduced to the corresponding relative quantities

$$\frac{\Delta I}{I} = \frac{I_E - I_0}{I_0}, \tag{2}$$

where I_E is the intensity measured with an applied E-field and I_0 is the zero-field intensity. The measurements were repeated 10–30 times for each reflection in order to provide a Poisson error $\sigma_{\Delta I/I} = 2/n^{1/2}$ of less than $0.2-0.3\%$, where n is the total number of counts collected for each reflection.

Typically, 10–15 reflections can be measured during 1 week of beam time using a point detector. In total, we measured 54 reflections for α-GaPO$_4$ during four measurement sessions (4 weeks of beamline time). The relative diffraction intensity variation, averaged over all measured reflections, $\langle|\Delta I/I|\rangle$, was 0.58%, with the mean standard uncertainty $\langle\sigma(\Delta I/I)\rangle$ equal to 0.11%. For a few reflections with an optimum wavelength close to the $K_{\rm Ga}$-absorption edge, the $\Delta I/I$ value reached more than 3%. The averaged relative standard uncertainty $\varepsilon = \langle[\sigma(\Delta I/I)/|\Delta I/I|]\rangle$ resulted in 21% and can be considered as a reasonable characteristic of the experimental data precision.

Typical rocking curves of a reflection measured for positive, negative and zero values of an external E-field are shown in Fig. 2.[1]

In addition to the above E-field measurements, we performed an E-field-free X-ray diffraction experiment at room temperature. This was done to get information about atomic positions and the Debye–Waller factors of the crystal without an external electric field. Here a cube of 50 µm in size was cut from one of the wafers and the intensities of 333 independent high-angle reflections [$0.65 < \sin\theta/\lambda < 0.75$ Å^{-1} (34 reflections), $0.95 < \sin\theta/\lambda < 1.05$ Å^{-1} (27 reflections) and $1.28 < \sin\theta/\lambda < 1.33$ Å^{-1} (272 reflections)] were collected. The refinement of the atomic positional parameters and the elements of the atomic displacements tensor, U^{ij}, was carried out with the program *MOLDOS97* (Protas, 1997; Hansen & Coppens, 1978); it resulted in R factors of $R = 0.011$, $R_w = 0.013$ and goodness of fit $S = 0.99$. The thermal displacement parameters are in good agreement with the results of previous X-ray diffraction studies of α-GaPO$_4$ (Baumgartner *et al.*, 1984; Litvin *et al.*, 1987).

3. The models for the data analysis

In paper I, we considered a structural model representing a crystal as a set of coupled harmonically vibrating rigid pseudoatoms (general model), which is most suitable for the analysis of a crystal response to an external permanent E-field on the atomic scale. We have found that the main contribution to the change in X-ray diffraction intensity results from the internal displacement of pseudoatoms, $\Delta\mathbf{R}_\mu$, where μ enumerates the symmetry-independent pseudoatoms within a unit cell. The relationship between the internal pseudoatomic displacements and microscopic parameters of a crystal can be written as

$$\Delta\mathbf{R}_\mu = \sum_{\alpha(\mathbf{q}_\alpha=\mathbf{0})} \sum_\nu \frac{Q_\nu(\mathbf{E}\mathbf{e}_{\nu\alpha})\mathbf{e}_{\mu\alpha}}{\omega_\alpha^2(m_\mu m_\nu)^{1/2}}. \tag{3}$$

Here Q_ν is the charge of the pseudoatomic fragment, $\mathbf{e}_{\mu\alpha}$, ω_α and $\mathbf{q}_\alpha$ are the polarization vectors, frequencies and wavevectors, respectively, of a specific phonon mode α; m_μ is a nuclear mass and $\mathbf{E}$ is the vector of the external electric field. The structure factor of a crystal in an external E-field is

$$F_E(\mathbf{H}) = \sum_\mu [f_\mu(\mathbf{H}) + f'_\mu(\lambda) + if''_\mu(\lambda)]T_\mu(\mathbf{H})\exp(2\pi i\mathbf{H}\mathbf{R}_\mu) \times \exp[2\pi i\mathbf{H}\Delta\mathbf{R}_\mu(\mathbf{E})], \tag{4}$$

where $\mathbf{H}$ is the scattering vector, $f_\mu(\mathbf{H})$, $T_\mu(\mathbf{H})$ are the atomic scattering and temperature factors, respectively, $\mathbf{R}_\mu$ are the equilibrium positions of the pseudoatoms without an external E-field, the sum is taken over the atoms within a unit cell. Anomalous dispersion is taken into account as corrections to atomic scattering factors.

In the kinematical approximation for X-ray diffraction, the scattering intensity is proportional to the square of the structure factor. The relative variation of the diffraction intensity in an external E-field in this case is

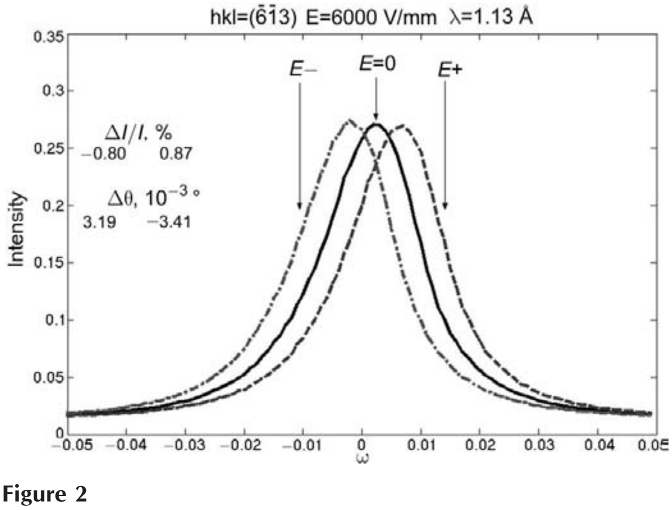

Figure 2
The typical change of a rocking curve induced by a permanent external E-field.

---

[1] The measured $\Delta I/I$ values, and the measured and simulated values of the relative diffraction intensity variations are available from the IUCr electronic archives (Reference: SH5033). Services for accessing these data are described at the back of the journal.

$$\frac{\Delta I}{I} = \frac{|F_E(\mathbf{H})|^2 - |F_{E=0}(\mathbf{H})|^2}{|F_{E=0}(\mathbf{H})|^2}. \tag{5}$$

The quantities (5) are measured in the experiment and should be compared with the corresponding simulated values. The variations of diffraction intensity can be calculated on the basis of field-free parameters (atomic positions, Debye–Waller and atomic form factors) and a specific model for the pseudoatomic displacements, induced by the static external E-field. We used the results of our X-ray diffraction experiment (see §2) to get the information on the crystal structure without an external electric field.

For convenience, let us decompose the vector quantities in expression (3) by the direct and reciprocal crystal-lattice vectors. Denoting by the superscript index x^i the vector components with respect to the direct basis vectors and with the subscript x_i its components with respect to the reciprocal basis vectors, one can rewrite (3) in the coordinate form:

$$\Delta R^i_\mu = \sum_j a^i_j(\mu) E^j. \tag{6}$$

The matrix elements $a^i_j(\mu)$ are considered as model parameters and refined by fitting the model of relative intensity variations to the experimental ones. They characterize the displacement of the μth atom along the ith crystallographic axis, induced by the 1 kV mm^{-1} external E-field parallel to the jth crystallographic axis. From expressions (3) and (6), the quantities $a^i_j(\mu)$ are related to the microscopic structural parameters and the elements of a dynamical matrix, D, in the centre of a Brillouin zone (Born & Huang, 1954):

$$a^i_j(\mu) = \sum_{\alpha(\mathbf{q}_\alpha=0)} \sum_\nu \frac{Q_\nu e^i_{\mu\alpha} e_{\nu\alpha j}}{\omega^2_\alpha (m_\mu m_\nu)^{1/2}} = \sum_\nu \frac{Q_\nu [D^i_j(\mu\nu)]^{-1}}{(m_\mu m_\nu)^{1/2}}. \tag{7}$$

The total number of model parameters is defined by the number of symmetry-independent atoms in a unit cell. If the displacement of the μth pseudoatom is described by a displacement tensor $\hat{\mathbf{a}}(\mu)$, then the response of a symmetry-equivalent atom, μ_s, to an external E-field will be described by the tensor

$$\hat{\mathbf{a}}(\mu_S) = \hat{\mathbf{S}}\hat{\mathbf{a}}(\mu)\hat{\mathbf{S}}^{-1}, \tag{8}$$

where $\mathbf{S}$ is a rotation matrix of the corresponding symmetry operation. For the atoms occupying special positions ($\mu_s = \mu$), expression (8) is considered as an additional constraint, related to their local symmetry. As a result, for the α-GaPO$_4$ structure, one can get the following elements of the displacement matrices to be refined on the basis of measured diffraction intensity variations:

$$\mathrm{Ga}: \begin{bmatrix} a^1_1(\mathrm{Ga}) & a^1_2(\mathrm{Ga}) & a^1_3(\mathrm{Ga}) \\ 0 & a^1_1(\mathrm{Ga}) + 2a^1_2(\mathrm{Ga}) & 2a^1_3(\mathrm{Ga}) \\ 0 & a^3_2(\mathrm{Ga}) & a^3_3(\mathrm{Ga}) \end{bmatrix} \tag{9a}$$

$$\mathrm{O1}: \begin{bmatrix} a^1_1(\mathrm{O1}) & a^1_2(\mathrm{O1}) & a^1_3(\mathrm{O1}) \\ a^2_1(\mathrm{O1}) & a^2_2(\mathrm{O1}) & a^2_3(\mathrm{O1}) \\ a^3_1(\mathrm{O1}) & a^3_2(\mathrm{O1}) & a^3_3(\mathrm{O1}) \end{bmatrix} \tag{9b}$$

$$\mathrm{P}: \begin{bmatrix} a^1_1(\mathrm{P}) & a^1_2(\mathrm{P}) & a^1_3(\mathrm{P}) \\ 0 & a^1_1(\mathrm{P}) + 2a^1_2(\mathrm{P}) & 2a^1_3(\mathrm{P}) \\ 0 & a^3_2(\mathrm{P}) & a^3_3(\mathrm{P}) \end{bmatrix} \tag{9c}$$

$$\mathrm{O2}: \begin{bmatrix} a^1_1(\mathrm{O2}) & a^1_2(\mathrm{O2}) & a^1_3(\mathrm{O2}) \\ a^2_1(\mathrm{O2}) & a^2_2(\mathrm{O2}) & a^2_3(\mathrm{O2}) \\ a^3_1(\mathrm{O2}) & a^3_2(\mathrm{O2}) & a^3_3(\mathrm{O2}) \end{bmatrix}. \tag{9d}$$

We should however take into account the particular wafer orientation in our experiment, where the electric-field vectors are always in the hexagonal plane. Therefore the pseudoatomic displacements induced by the c component of an external E-field, *i.e.* the third columns of the matrices in (9) are not available from the experiments performed in this work. Moreover, the fact that the quantities $|F_E(\mathbf{H})|^2$ depend on the relative positions of the atoms within the unit cell leads to an additional constraint, which can be expressed as

$$\sum_\mu \Delta\mathbf{R}_\mu(\mathbf{E}) = 0 \tag{10}$$

or, in terms of the atomic displacement matrix, as

$$\sum_{\mu(\mathrm{ind})} \sum_s a^i_j(\mu, s)/s_\mu = 0. \tag{11}$$

Here the first summation is only carried out over the symmetry-independent pseudoatoms and the second one over all symmetry operations. The factor s_μ takes into account the multiplicity of the point group, corresponding to the position of the μth atom: in α-GaPO4, $s_\mu = 1$ for O atoms, $s_\mu = 2$ for Ga and P atoms. After the summation over the symmetry operations, expression (10) can be transformed into the following form:

$$\sum_\mu [a^1_1(\mu) + a^2_2(\mu)]/s_\mu = 0. \tag{12}$$

This constraint reduces the effective number of model parameters by one. Finally, the total number of free parameters that should be determined with α-GaPO$_4$ in the general model is 17.

In addition to the general model of pseudoatomic displacements, we can consider two simplified models based on specific assumptions for the phonon spectrum of a crystal lattice. The first model assumes that atoms in the crystal vibrate independently of each other (model of independent atomic vibrations, IVAM, see paper I). Expression (7) can then be transformed into

$$a^i_j(\mu) = \frac{Q_\mu \beta^{ik} g_{kj}}{2\pi^2 k_B T}. \tag{13}$$

Table 1
The crystal structural parameters of α-GaPO$_4$ obtained from the high-angle X-ray diffraction experiment without an electric field.

Crystal lattice parameters (hexagonal setting)	
a (Å)	4.9025 (1)
c (Å)	11.0526 (2)
V (Å^3)	229.817

Positions of symmetry-independent atoms (space group $P3_121$) (fractional coordinates)

	Ga	O1	P	O2
R^1	0.45633 (2)	0.40865 (18)	0.45655 (5)	0.40934 (16)
R^2	0.00000	0.31827 (17)	0.00000	0.27328 (17)
R^3	0.33333	0.39221 (5)	0.83333	0.87188 (4)

Thermal vibration parameters [temperature factor is $T_\mu(\mathbf{H}) = \exp(-2\pi^2 \sum_{ij} a^i a^j U^{ij} h_i h_j)$, a^i are reciprocal-lattice parameters]

	Ga	O1	P	O2
U^{11} (10^{-2} Å^2)	0.856 (4)	1.835 (17)	0.834 (5)	1.935 (18)
U^{22} (10^{-2} Å^2)	0.706 (3)	1.347 (11)	0.615 (5)	1.237 (11)
U^{33} (10^{-2} Å^2)	0.688 (2)	1.162 (10)	0.656 (5)	1.249 (12)
U^{12} (10^{-2} Å^2)	$1/2U^{22}$	1.084 (11)	$1/2U^{22}$	1.089 (13)
U^{13} (10^{-2} Å^2)	$1/2U^{23}$	−0.395(10)	$1/2U^{23}$	−0.483 (11)
U^{23} (10^{-2} Å^2)	−0.055 (1)	−0.443 (8)	−0.041 (3)	−0.445 (8)

Here k_B is the Boltzmann constant, T is the absolute temperature, β^{ik} is a thermal displacement tensor, g_{ij} is a metric tensor of a crystal lattice. In principle, all these quantities can be known before starting an X-ray diffraction experiment in the presence of the external E-field: the elements of the thermal displacements tensors, β^{ij}, can be derived from X-ray diffraction structure analysis (at zero external E-field); pseudoatomic charges, Q_μ, can be estimated using a multipole-model refinement of the crystal electron density or density functional theory (DFT) calculations. Thus, expression (13) can be applied to get *a priori* estimations of both the pseudoatomic displacements and the relative changes in X-ray diffraction intensities induced by an external E-field. Note, however, that exact values of pseudoatomic charges, Q_μ, are not available since the decomposition of electron density into a sum of rigid pseudoatomic fragments is ambiguous. Therefore the quantities Q_μ in (13) may be considered as model parameters, constrained by the condition of the electroneutrality of a unit cell.

$$\sum_{\mu(\text{ind})} Q_\mu / s_\mu = 0. \tag{14}$$

Taking into account the number of symmetry non-equivalent atoms and the condition (14), one can see that the total number of independent parameters of the IVAM for α-GaPO$_4$ is three.

The second simplified model is related to the Meissner model, introduced in 1927 (Meissner, 1927), which is discussed in a number of textbooks describing piezoelectric effect and dielectric polarization in quartz-related materials. It is based on the assumption that the pseudoatomic displacements are always parallel or antiparallel to the external E-field and yields

$$\Delta\mathbf{R}_\mu = a_\mu \mathbf{E}. \tag{15}$$

Table 2
Summary of pseudoatomic displacement models used in the refinements; N is the number of free model parameters.

Model	Displacement expression	Constraints	N
General	$\Delta R^i_\mu = a^i_j(\mu) E^j$	$\sum_\mu [a^1_1(\mu) + a^2_2(\mu)]/s_\mu = 0$ + symmetry constraints	17
IVAM	$\Delta R^i_\mu = Q_\mu \beta^{ik} g_{kj} E^j / 2\pi^2 k_B T$	$\sum_\mu Q_\mu / s_\mu = 0$	3
Meissner model	$\Delta\mathbf{R}_\mu = a_\mu \mathbf{E}$	$a_1 = 0$ (fixed origin at Ga atom)	3

This model can be derived by replacing the frequencies of phonon vibrations in equation (7) by an average value $\omega_\alpha \approx \omega$, typical of the average frequency of optical phonon modes, and then taking into account the orthogonality condition for the phonon polarization vectors, $\sum_\alpha e^i_{\mu\alpha} e_{\nu\alpha j} = \delta^i_j \delta_{\mu\nu}$. In this case, equation (7) transforms into

$$a^i_j(\mu) = \frac{Q_\mu \delta^i_j}{m_\mu \omega^2}. \tag{16}$$

The coefficients a_μ are refined in the Meissner model; they have the same values for symmetry-equivalent atoms. The total number of independent parameters for α-GaPO$_4$ is equal to 3, since the origin must be fixed at one of the atoms.

4. Determination of model parameters from the relative intensity variations

We used all models mentioned above to determine the values of the model parameters, which are found by minimizing the error sum functional

$$f = \sum_i \left[\frac{(\Delta I/I)_{i\text{OBS}} - (\Delta I/I)_{i\text{MOD}}}{\sigma(\Delta I/I)_i} \right]^2, \tag{17}$$

where $(\Delta I/I)_{i\text{OBS}}$ and $(\Delta I/I)_{i\text{MOD}}$ are the observed and model values of the relative diffraction intensity variations, respectively. The values for the X-ray diffraction intensity variations are modelled on the basis of expressions (4) and (5). The structural information and the models of pseudoatomic displacements (see §3) are given in Table 1 and Table 2.

For the minimization of the error sum, we have used a constrained algorithm (Powell, 1978) implemented in the *MATLAB* program package (*fmincon* function). This method utilizes sequential quadratic programming to solve the general problem of a function minimization under specific constraints, presented in the form of equations or inequalities.

The quality of a fit was estimated by calculating agreement indices (weighted and unweighted R factors) for the relative diffraction intensity variations defined as

$$\begin{aligned} R_w &= \left[\frac{\sum_i w_i [(\Delta I/I)_{i\text{OBS}} - (\Delta I/I)_{i\text{MOD}}]^2}{\sum_i w_i [(\Delta I/I)_{i\text{OBS}}]^2} \right]^{1/2} \\ R &= \frac{\sum_i |(\Delta I/I)_{i\text{OBS}} - (\Delta I/I)_{i\text{MOD}}|}{\sum_i |(\Delta I/I)_{i\text{OBS}}|}. \end{aligned} \tag{18}$$

The weights, w_i, are related to the standard uncertainties by $w_i = 1/\sigma(\Delta I/I)_i^2$. The reliability factors, defined in this way, are normalized to 100%, *i.e.* they take the value of 1 for zero pseudoatomic displacements $[(\Delta I/I)_{i\mathrm{MOD}} = 0]$.

The indices of the model fit over the 54 measured reflections are shown in Table 3. It is evident that both the Meissner model and the IVAM model provide a poor fit to the experimental intensity variations. On the other hand, the general model results in $R_w = 0.18$, which is even smaller than the average relative standard uncertainty of the measured values, $\langle|\sigma/(\Delta I/I)|\rangle = 0.21$. In this sense, all the solutions with weighted R factors less than 0.21 can be considered as reasonable ones. Unfortunately, several different sets of displacement parameters resulting in R factors smaller than 0.21 were found. It requires an additional, physically motivated, constraint to find the correct displacements of pseudoatoms induced by the permanent external E-field. We shall consider such a constraint in the next section.

Table 3
The values of an error sum and R factors, obtained with different models of pseudoatomic displacements induced by an external E field.

Model	Error sum	R_w	R
Meissner	3079	0.424	0.423
IVAM	2168	0.356	0.350
General without constraint	548	0.179	0.172
General with constraint (dielectric polarization)	754	0.210	0.190

5. Dielectric polarization derived from pseudoatomic displacements

Let us analyse the pseudoatomic displacements, obtained within the general model, in terms of the macroscopic polarization of a crystal. The rigid pseudoatomic model for the crystal electron density allows us to write the following expression for the polarization vector of a crystal unit cell induced by an external E-field:

$$\Delta P_i = \sum_{\mu(\mathrm{ind})} Q_\mu/s_\mu \sum_s a_{ij}(\mu, s)E_j/V, \qquad (19)$$

where V is the volume of a crystal unit cell. The vector and tensor quantities in (19) are expressed in a Cartesian coordinate system, associated with the hexagonal crystallographic setting (Nye, 2004).

One can suppose that the dielectric polarization is homogeneous throughout the crystal space, including the surface, and then vanishes outside the crystal. Under this assumption, the dielectric polarization, ΔP_i, of a unit cell can be identified with the dielectric polarization of all the crystal. The macroscopic theory (Lines & Glass, 1979) relates it to the vector of the external electric field by the tensor of dielectric susceptibility, of a crystal medium, ε_{ij}, and the vacuum susceptibility, ε_0:

$$\Delta P_i = \varepsilon_0(\varepsilon_{ij} - \delta_{ij})E_j. \qquad (20)$$

The independent dielectric constants for α-GaPO$_4$, $\varepsilon_{11} = \varepsilon_{22} = 6.2$ and $\varepsilon_{33} = 6.6$, are taken from Foulon *et al.* (1994).

Using (19) and (20), one can express the tensor of dielectric susceptibility *via* the microscopic model parameters:

$$\varepsilon_{ij}^{(\mathrm{exp})} = \delta_{ij} + \sum_{\mu(\mathrm{ind})} Q_\mu/s_\mu \sum_s a_{ij}(\mu, s)/(\varepsilon_0 V). \qquad (21)$$

One can require that the physically correct pseudoatomic displacements have to provide the correct values of the dielectric matrix of the compound (see above). In the present work, we use this condition as an additional constraint for the refinement of the general model. Because in our experiment the electric field was always applied within the hexagonal plane of a crystal lattice, the third column of a dielectric matrix could not be determined from our experiment.

The pseudoatomic charges Q_μ have been calculated according to Bader's (1990) topological theory of the electron density. The calculation of the ground-state electron density of α-GaPO$_4$ was performed using the density functional theory approach as implemented in the program package *WIEN2k* (Blaha *et al.*, 2001), which utilizes 'an augmented plane waves plus local orbitals' method. The calculation converged with small values of atomic forces less than 1 mRy a.u.$^{-1}$. The atomic charges obtained by integration over the zero-flux atomic basins (Bader, 1990) are $Q_{\mathrm{Ga}} = 1.77$, $Q_{\mathrm{P}} = 3.13$, $Q_{\mathrm{O1}} = -1.22$, $Q_{\mathrm{O2}} = -1.23$ e.

Evaluating the sum over symmetry operations, one can rewrite (21) in the following form:

$$\varepsilon_{11}^{(\mathrm{exp})} = 1 + 3\sum_{\mu(\mathrm{ind})} Q_\mu/s_\mu[a_1^1(\mu) + a_2^2(\mu)]/(\varepsilon_0 V), \qquad (22)$$

therefore the application of the above constraint leads to the reduction of the number of independent parameters by 1. The total number of independent parameters refined from the experimental data is 16.

Under the condition $\varepsilon_{11}^{(\mathrm{exp})} = \varepsilon_{11}$, the functional (16) approaches a global minimum, characterized by the weighted R factor, $R_w = 0.21$. It now has the same value as an averaged relative standard uncertainty of observations, therefore our obtained solution can be considered as satisfactory for the present experimental data. At the same time, it reflects physically meaningful results. Table 4 lists the resulting values for the elements of displacement matrices of symmetry-independent atoms along with the 16 standard uncertainties of refined elements. The displacement matrices of the symmetry-equivalent atoms are calculated on the basis of equation (8). The corresponding displacements of pseudoatoms in α-GaPO$_4$ induced by an electric field (1 kV mm^{-1}) parallel to the [110] direction are given in Table 5.[2] Note that the values for the atomic displacement can change slightly if the pseudoatomic charges are calculated in another way.

---

[2] See deposition footnote.

Table 4
The elements of displacement matrices, refined on the basics of a general model with constraint; the elements of the third columns cannot be determined from the experiment and are marked by ×.

Atom	a_j^i, 10^{-20} m^2 V^{-1}
Ga	$\begin{pmatrix} 0.581 & -0.177 & \times \\ 0 & 0.226\,(1) & \times \\ 0 & 0.012\,(1) & \times \end{pmatrix}$
O1	$\begin{pmatrix} 0.048\,(1) & -0.508\,(1) & \times \\ 0.033\,(1) & -0.339\,(2) & \times \\ -0.378\,(4) & 0.193\,(2) & \times \end{pmatrix}$
P	$\begin{pmatrix} 0.266 & -0.032 & \times \\ 0 & -0.201\,(1) & \times \\ 0 & 0.107\,(1) & \times \end{pmatrix}$
O2	$\begin{pmatrix} -0.020\,(1) & -0.473\,(3) & \times \\ 0.258\,(3) & -0.326\,(2) & \times \\ -0.143\,(2) & 0.412\,(4) & \times \end{pmatrix}$

Table 5
The displacements of pseudoatoms induced by an external *E*-field $\mathbf{E}$ = 1 kV mm^{-1} applied along the [110] direction (fractional coordinates).

	$\Delta\mathbf{R}^1$ ($\times10^{-5}$)	$\Delta\mathbf{R}^2$ ($\times10^{-5}$)	$\Delta\mathbf{R}^3$ ($\times10^{-5}$)
Ga1	0.824	0.462	0.025
Ga2	0.462	0.824	−0.025
Ga3	1.187	1.187	0.000
O11	−0.940	−0.624	−0.378
O12	−0.693	0.345	−0.395
O13	0.031	0.100	0.773
O14	−0.624	−0.939	0.378
O15	0.345	−0.693	0.395
O16	0.100	0.031	−0.773
P1	0.477	0.411	0.219
P2	0.411	0.477	−0.219
P3	0.542	0.542	0.000
O21	−1.007	−0.139	0.549
O22	−0.666	0.300	−0.841
O23	−0.569	−0.042	0.292
O24	−0.139	−1.007	−0.549
O25	0.300	−0.666	0.841
O26	−0.042	−0.569	−0.292

6. Discussion

A representation of structural variations in α-GaPO$_4$ induced by a permanent external *E*-field applied parallel to [110] is shown in Fig. 3 presenting the projection of a crystal structure on the hexagonal plane and in Fig. 4 showing the projection of a structure to the plane perpendicular to the external *E*-field. For the chosen direction of an external electric field, the symmetry of a distorted crystal is reduced to the symmetry group *C*2, with the twofold axis parallel to the electric field. The tetrahedra centred at Ga1 and Ga2 as well as at P1 and P2 atoms are related to the corresponding symmetry operation. However, that would not be the case for an arbitrary direction of an electric field.

Fig. 3 shows that the shift of the cations (Ga, P) is almost aligned in the direction of the field. In contrast, the shift of each O atom does not exhibit a strong correlation to it. That suggests that an external *E*-field primarily influences the cation positions, while the displacements of anions approximately follow the movement of the cation in the centre of a corresponding tetrahedron. The strength of a chemical bond in the tetrahedral units influences the specific atomic shifts greatly; the *E*-field-induced structural modifications tend, in general, to keep the change of bond distances as small as possible.

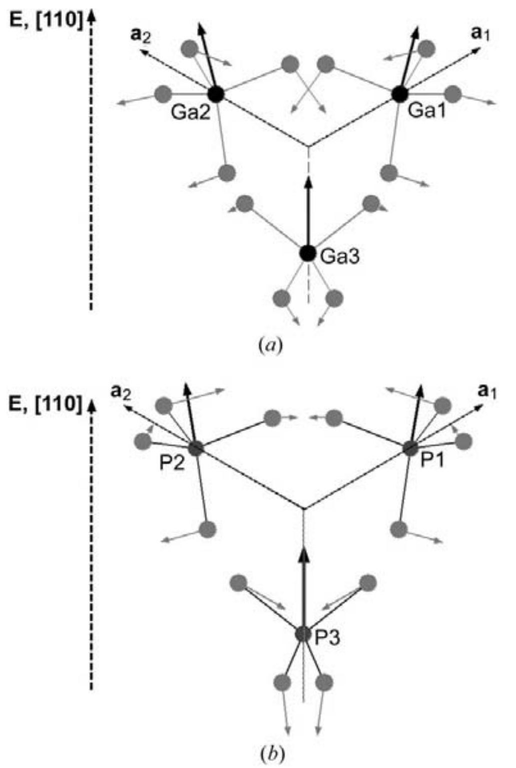

Figure 3
The displacements of pseudoatoms in (*a*) GaO$_4$ and (*b*) PO$_4$ sublattices induced by an external *E*-field parallel to the [110] lattice direction shown in projection on the hexagonal plane.

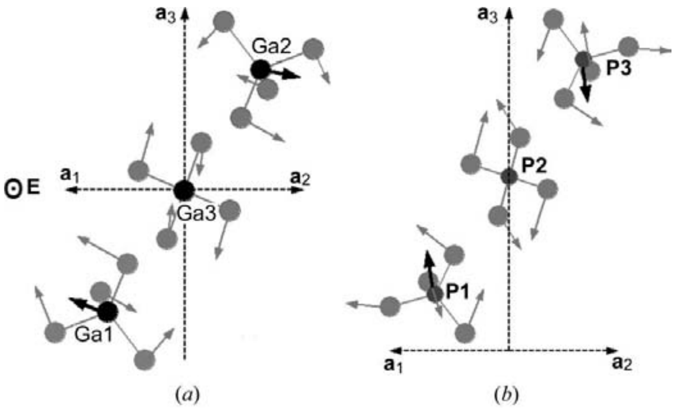

Figure 4
The displacements of pseudoatoms in (*a*) GaO$_4$ and (*b*) PO$_4$ sublattices induced by an external *E*-field, parallel to the [110] lattice direction shown in projection on the plane, perpendicular to the field direction.

Table 6
The distortion of the structural tetrahedra induced by an external electric field applied in the [110] crystallographic direction.

Tetrahedra	$\lambda_{M-\mathrm{O}}$ ($\times10^{-5}$)	$\lambda_{\mathrm{O-O}}$ ($\times10^{-5}$)	$\Delta\lvert\mathbf{p}_M\rvert$ (10^{-5} Å)	$\Delta V/V$ (10^{-3}%)
$[GaO_4]_1$	1.31	1.28	3.53	0.61
$[GaO_4]_2$	1.34	1.28	3.53	0.61
$[GaO_4]_3$	0.43	2.18	−7.06	−1.23
$[PO_4]_1$	2.30	1.76	2.66	−1.56
$[PO_4]_2$	2.30	1.76	2.66	−1.56
$[PO_4]_3$	3.25	1.44	−5.32	3.12

In order to quantify the structural changes, we have calculated the following electric-field-dependent quantities, related to the extent of distortion of the GaO_4 and PO_4 tetrahedra.

(i) The relative change of the cation–anion distances, d, averaged over each tetrahedron:

$$\lambda_{M-\mathrm{O}} = \sum_{\mathrm{tetra}} \left\langle \left| \frac{\Delta d_{M\mathrm{O}_i}}{d_{M\mathrm{O}_i}} \right| \right\rangle \Big/ 4, \quad M = \mathrm{Ga, P}. \tag{23}$$

(ii) The relative change of anion–anion distances, averaged over one tetrahedron:

$$\lambda_{\mathrm{O-O}} = \sum_{\mathrm{tetra}} \left\langle \left| \frac{\Delta d_{\mathrm{OO}}}{d_{\mathrm{OO}}} \right| \right\rangle \Big/ 6. \tag{24}$$

(iii) The change of the tetrahedron distortion vector, $\Delta|\mathbf{p}_M|$ (Guillot, 2002), where the tetrahedron distortion vector itself is defined as

$$\mathbf{p}_M = \sum_{i=1}^{4} \mathbf{R}_{\mathrm{O}_i}/4 - \mathbf{R}_M, \quad M = \mathrm{Ga, P}. \tag{25}$$

(iv) The relative change of the volume of a tetrahedron induced by an external E-field, $\Delta V/V$.

The above parameters, normalized to $E = 1$ kV mm^{-1}, with **E**//[110], are listed in Table 6.

The relative change of cation–anion distances (the first parameter) is most informative for description of the distortion of individual bonds in a tetrahedron. It can be considered as a major property for performing bond-type selective analysis of different bond-length changes. We find approximately 1.5 times stronger distortion of the bonds in the PO_4 tetrahedron compared with GaO_4.

The difference in the change of distances (the second parameter) between various O atoms within the GaO_4 and PO_4 tetrahedra is less pronounced; however, it is more influenced by the neighbouring structural units, since each O atom is shared by two neighbouring tetrahedra.

The change of the tetrahedra deformation vector (the third parameter) characterizes the deviation of a structural unit from its regular form: for the regular tetrahedron with the cation at the geometrical centre, the distortion vector is zero. Note that in α-$GaPO_4$ both types of structural units (GaO_4 and PO_4) are already slightly distorted without an applied field. The length of a distortion vector without an E-field was found to be 0.0146 Å for GaO_4 tetrahedra and 0.0135 Å for PO_4 tetrahedra. The field-induced deviation from regularity, given in Table 6 (column 3), shows that PO_4 tetrahedra tend to keep a more regular form than GaO_4 tetrahedra.

The relative change in the tetrahedron volumes (the fourth parameter) differs by a factor of three. As seen in Table 6, the response of a particular GaO_4 or PO_4 tetrahedron depends on its relative position within the unit cell. For the given direction of the E-field, the tetrahedra centred at the Ga1 and Ga2 atoms tend to be stretched, while the tetrahedra centred at the Ga3 site are compressed. The distortion of the P tetrahedron exhibits the opposite tendency, the structural units based on the P1 and P2 atoms are squeezed while the tetrahedra centred on the P3 atom are stretched.

The established distortion of the α-$GaPO_4$ structure owing to an external electric field is proved to be statistically significant. To demonstrate this, we performed a constrained minimization for a number of reflections less than 54 and calculated the corresponding $\lambda_{M-\mathrm{O}}$ values averaged over all the GaO_4 and PO_4 tetrahedra. The dependence of the tetrahedron distortion parameter on the number of reflections is given in Fig. 5. It shows that our solution is stable enough and the tetrahedron distortion does not critically depend on the number of reflections used.

To clarify the nature of the behaviour of the GaO_4 and PO_4 tetrahedra, let us consider their distortions in the E-field as a result of a competition of the purely covalent and purely ionic responses of a structure to the external electric field. The ionicity of a chemical bond can be roughly estimated by considering the difference between electronegativities, χ_i, of bonded atoms (Pauling, 1939). On the Pauling scale, the values of electronegativity for the Ga, P and O atoms are $\chi_{\mathrm{Ga}} = 1.6$, $\chi_{\mathrm{P}} = 2.1$ and $\chi_{\mathrm{O}} = 3.5$, respectively, therefore the electronegativity differences lead us to a conclusion that the Ga—O chemical bond has larger ionicity compared with the P—O one. This conclusion is in good agreement with results of the calculation performed by Defregger *et al.* (1991) in the framework of Levine's bond-charge model (Levine, 1973). According to Defregger *et al.* (1991), the ionicity of the Ga—O bond in α-$GaPO_4$ is 0.64 while the ionicity of the P—O bond is 0.46.

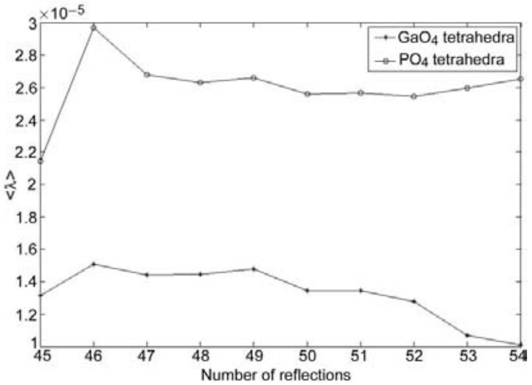

Figure 5
The dependence of the tetrahedra distortion parameter on the number of reflections included in the refinement.

Using the DFT wavefunction, we have also performed a topological analysis of the electron density, which considers the features of the electron density itself, the Laplacian of the electron density, the kinetic, potential and total electronic energy densities (Bader, 1990; Tsirelson & Ozerov, 1996). Consideration of these functions at the bond critical points allows one to associate the bonds with the closed-shell, shared interactions or intermediate atomic interactions. According to Macchi *et al.* (1998), Tsirelson (1999), Bianchi *et al.* (2000), Espinosa *et al.* (2002), Macchi & Sironi (2003), Marabello *et al.* (2004), Stash *et al.* (2005) and Gatti (2005), both the Ga—O and P—O interactions are intermediate ones, the Ga—O bond is closer to the ionic limit, while the P—O bond has a more pronounced covalent component (Table 7). The strength of the chemical bond is described by the quantity h_e/ρ (Espinosa *et al.*, 2002), where h_e and ρ are the electronic energy density and the electron density at the bond critical point, respectively. In the case of α-GaPO$_4$, the stronger the interaction, the more negative the h_e/ρ magnitude. Table 7 shows that, in terms of the topological analysis of the electron density, the P—O bond in α-GaPO$_4$ is stronger compared to the Ga—O bond.

From all these points of view, the chemical bonds in α-GaPO$_4$ have a dominant ionic character. Thus, the key quantities, defining the distortion of the structural units owing to the electric field, are the atomic charges: the electrostatic forces, tending to deform the tetrahedra in α-GaPO$_4$, are proportional to the atomic charges. At the same time, the covalent chemical bond is related to the electron-density distribution between bonded atoms. The latter is responsible for the forces tending to keep the tetrahedra undistorted by the applied electric field. The competition of the two forces is implicitly described by equation (7) relating *E*-field-induced displacements of the μth pseudoatom with the pseudoatomic charges of all atoms in the unit cell and the forces between them. The covalency of a chemical bond between neighbouring atoms influences the non-diagonal terms of the matrix, $Q_\nu[D^{ij}(\mu \neq \nu)]^{-1}$, while the diagonal elements $Q_\mu[D^{ij}(\mu\mu)]^{-1}$ account for the ionic contribution to the atomic displacements.

Taking into account the results listed in Table 7 and the pseudoatomic charges $Q_{\rm Ga} = 1.77$, $Q_{\rm P} = 3.13$, $Q_{\rm O1} = -1.22$, $Q_{\rm O2} = -1.23$ e, we can conclude that the larger distortion of the PO$_4$ tetrahedron induced by the permanent external *E*-field results from a larger value of the pseudoatomic charge of the P atom and, consequently, larger electrostatic forces deforming this tetrahedron. The strength of the P—O bond (which is larger than the Ga—O bond) is not strong enough to prevent the distortion of the PO$_4$ tetrahedron in an external *E*-field.

It would be reasonable to compare our results with the results of other experiments taken under non-ambient conditions. The X-ray diffraction under high pressure looks a good choice for such comparison. Unfortunately, the only available study of α-GaPO$_4$ (Sowa, 1994) under high pressure did not allow the site-selective analysis of the GaO$_4$ and PO$_4$ tetrahedra to be established.

Table 7
The topological features of the bond critical points for the chemical bonds in the GaO$_4$ and PO$_4$ tetrahedra.

$\rho_{\rm BCP}$ is an electron density, $\nabla^2\rho_{\rm BCP}$ is a Laplacian of electron density, g, v and $h_e = v + g$ are the kinetic, potential and total electronic energy densities, respectively. Atomic units are used.

Bond	$\rho_{\rm BCP}$	$\nabla^2\rho_{\rm BCP}$	g	v	h_e	$\|v\|/g$	$g/\rho_{\rm CP}$	$h_e/\rho_{\rm BCP}$
Ga—O	0.124	0.56	0.18	−0.22	−0.04	1.23	1.46	−0.32
P—O	0.218	0.77	0.35	−0.52	−0.17	1.46	1.63	−0.73

Hazen & Downs (2000) in a number of high-pressure diffraction studies have revealed that the distortion of a coordination polyhedron, to a first approximation, is independent of the particular crystal structure. In a similar way, one can suppose that the distortion of tetrahedral units in the external electric field will be only slightly dependent on the specific crystal structure. It might be interesting to verify this supposition in the future by studying other compounds with the GaO$_4$ and PO$_4$ structural units under external electric field.

In summary, in the present study, we have determined the pseudoatomic displacement in α-GaPO$_4$ induced by an external strong electric field. Similar to α-quartz (Davaasambuu, 2003; Guillot *et al.*, 2004), the crystal *E*-field response in α-GaPO$_4$ cannot be described by the classical Meissner model but by distortions of *M*O$_4$ (*M* = Ga, P) structural units. The strength of the tetrahedron distortion scales with the ratio between the covalent and ionic character of the chemical bond. For the first time, we have performed site-selective analysis of the *E*-field-induced distortion of a ternary crystal structure, here the distortion of PO$_4$ and GaO$_4$ tetrahedra in α-GaPO$_4$, and interpreted the bond distortions in terms of specific features of charge density and the pseudoatomic charges of this material.

This project has been supported by DFG under Priority program 1178. VT thanks the Alexander von Humboldt Foundation for support in the form of the Scientific Award. The authors thank N. K. Hansen (Nancy) for fruitful discussions.

References

Aslanov, L. A., Trunov, V. A., Fetisov, G. V., Priemyshev, V. A., Rybakov, V. B., Kasman, Ya. A. & Bulkin, A. P. (1989). *J. Appl. Cryst.* **22**, 42–45.

Bader, R. F. W. (1990). *Atoms in Molecules: a Quantum Theory* Oxford University Press.

Baumgartner, O., Preisinger, A., Krempl, P. W. & Mang, H. (1984) *Z. Kristallogr.* **168**, 83–91.

Bianchi, R., Gervasio, G. & Marabello, D. (2000). *Inorg. Chem.* **39**, 2360–2366.

Blaha, P., Schwarz, K., Madsen, G. K. H., Kvasnicka, D. & Luitz, J. (2001). *WIEN2k. An Augmented Plane Wave + Local Orbital Program for Calculating Crystal Properties.* Technical Universität, Wien, Austria.

Born, M. & Huang, K. (1954). *Dynamical Theory of Crystal Lattices.* Oxford: Clarendon Press.

Coppens, P. (1997). *X-ray Charge Densities and Chemical Bonding.* New York: Oxford University Press.

Davaasambuu, J. (2003). PhD thesis, Potsdam University.

Davaasambuu, J., Pucher, A., Kochin, V. & Pietsch, U. (2003). *Europhys. Lett.* **62**, 834–840.

Defregger, S., Engel, G. F. & Krempl, P. W. (1991). *Phys. Rev. B*, **43**, 6733–6738.

Espinosa, E., Alkorta, I., Elguero, J. & Molins, E. (2002). *J. Chem. Phys.* **117**, 5529–5542.

Foulon, J. D., Giuntini, J. C. & Philippot, E. (1994). *Eur. J. Solid State Inorg. Chem.* **31**, 245–256.

Fujimoto, I. (1982). *Acta Cryst.* A**38**, 337–345.

Gatti, C. (2005). *Z. Kristallogr.* **220**, 399–457.

Glinnemann, J., King, H. E., Schultz, H., Hahn, T., Placa, S. J. L. & Dacol, F. (1992). *Z. Kristallogr.* **198**, 177–212.

Gorfman, S., Tsirelson, V. & Pietsch, U. (2005). *Acta Cryst.* A**61**, 387–396.

Graafsma, H., Coppens, P., Majewski, J. & Cahen, D. (1992). *J. Solid State Chem.* **105**, 520–527.

Graafsma, H., Heunen, G. W. J. C. & Schulze, C. (1998). *J. Appl. Cryst.* **31**, 414–422.

Guillot, R. (2002). PhD thesis, University Henri Poincaré, Nancy, France.

Guillot, R., Fertey, P., Hansen, N. K., Alle, P., Elkaim, E. & Lecomte, C. (2004). *Eur. Phys. J.* B**42**, 373–380.

Hansen, N. K. & Coppens, P. (1978). *Acta Cryst.* A**34**, 909–921.

Hazen, R. M. & Downs, R. T. (2000). *High Temperature and High Pressure Crystal Chemistry.* Washington, DC: Mineralogical Society of America.

Hazen, R. M., Finger, L. W. Hemley, R. J. & Mao, H. K. (1989). *Solid State Commun.* **72**, 507–511.

Kochin, V., Davaasambuu, J., Pietsch, U., Schwarz, K. & Blaha, P. (2004). *J. Phys. Chem. Solids*, **65**, 1967–1972.

Krispel, F., Schleinzer, G., Krempl, P. W. & Wallnofer, W. (1997). *Ferroelectrics*, **202**, 307–311.

Levine, B. F. (1973). *Phys. Rev. B*, **7**, 2601–2625.

Lines, M. E. & Glass, A. M. (1979). *Principles and Applications of Ferroelectric and Related Materials.* Oxford: Clarendon Press.

Litvin, B. N., Popolitov, V. I., Simonov, M. A., Yakubovich, O. V. & Yaroslavskii, I. A. (1987). *Kristallografiya*, **32**, 486–489. (In Russian.)

Macchi, P., Proserpio, D. M. & Sironi, A. (1998). *J. Am. Chem. Soc.* **120**, 13429–13435.

Macchi, P. & Sironi, A. (2003). *Coord. Chem. Rev.* **238–239**, 383–412.

Marabello, D., Bianchi, R., Gervasio, G. & Cargnoni, F. (2004). *Acta Cryst.* A**60**, 494–501.

Meissner, A. (1927). *Z. Technol. Phys.* pp. 74–77.

Nye, J. (2004). *Physical Properties of Crystals and their Representation by Tensors and Matrices.* Oxford: Clarendon Press.

Pauling, L. (1939). *The Nature of the Chemical Bond and the Structure of Molecules and Crystals: an Introduction to Modern Structural Chemistry.* Ithaca, New York: Cornell University Press.

Powell, M. J. D. (1978). *Lecture Notes in Mathematics*, Vol. 630. Berlin: Springer Verlag.

Protas, J. (1997). *MOLDOS97/MOLLY* DOS updated version (private communications).

Puget, J. & Godefroy, L. J. (1975). *J. Appl. Cryst.* **8**, 297–303.

Reeuwijk, S. J. van (2002). PhD thesis, Twente University, The Netherlands.

Sowa, H. (1994). *Z. Kristallogr.* **209**, 954–960.

Stahn, J., Pietsch, U., Blaha, P. & Schwarz, K. (2001). *Phys. Rev. B*, **63**, 165205-1–10.

Stahn, J., Pucher, A., Geue, T., Daniel, A. & Pietsch, U. (1998). *Europhys. Lett.* **44**, 714–720.

Stash, A. I., Tanaka, K., Shiozawa, K., Makino, H. & Tsirelson, V. G. (2005). *Acta Cryst.* B**61**, 418–428.

Tsirelson, V. (1999). *Acta Cryst.* A**55** Supplement, Abstract M13.OF.003.

Tsirelson, V. G., Gorfman, S. V. & Pietsch, U. (2003). *Acta Cryst.* A**59**, 221–227.

Tsirelson, V. G. & Ozerov, R. P. (1996). *Electron Density and Bonding in Crystals.* Bristol, England/Philadelphia, USA: Institute of Physics Publishing.